Comparison of Thematic Mapper and NOARL Scanner Multispectral Bathymetry Estimates

AD-A226 273

M. T. Kalcic
C. L. Walker
H. V. Miller
Mapping, Charting, and Geodesy Division
Ocean Science Directorate

90 09 07 005

Foreword

The Naval Oceanographic and Atmospheric Research Laboratory's Mapping, Charting, and Geodesy Division performs research and development in new and improved methods for gathering navigational bathymetric data in coastal areas. One area of special interest is the development of algorithms to derive bathymetry from multispectral data. Currently, multispectral imagery can be derived from airborne scanners or from satellite sensors, such as the thematic mapper on board Landsat. Multispectral bathymetry has the potential for gathering data much more rapidly than present shipboard systems; in particular, satellite systems can gather data from many parts of the world that are denied to other collection systems. This report presents results in the use of different sources of multispectral data for bathymetry derivations.

W. B. Moseley
Technical Director

J. B. Tupaz, Captain, USN
Commanding Officer

Executive Summary

The Mapping, Charting, and Geodesy Division of the Naval Oceanographic and Atmospheric Research Laboratory (NOARL) investigates methods to exploit the application of multispectral data to coastal water mapping and charting requirements. The Coastal Image Understanding project high-resolution, multispectral, aircraft data has been examined and compared with lower-resolution satellite data from the thematic mapper on board NASA's Landsat. The high-resolution, nine-band scanner used was developed for the Airborne Bathymetric Survey System. The NOARL scanner has increased spectral sensitivity in the blue and green portions of the electromagnetic spectrum to take advantage of the water-penetrating bands. The multiband generalized ratio model is used to compare bathymetry estimates from the scanner and the thematic mapper, which has five bands. Results show improvement from increased resolution in the 3-m to 6-m area. Root-mean-square (RMS) errors of 0.323 m at the 3-m depth range for the NOARL Scanner are close to the International Hydrographic Office standard of 0.3 m; however, errors at other depth ranges exceed this standard. RMS errors of 0.544 m for the NOARL scanner contrast with 0.907 m for the thematic mapper at the 4-m range. Beyond 6-m depth, results do not differ significantly between the two scanners.

Acknowledgments

Contents

Comparison of Thematic Mapper and NOARL Scanner Multispectral Bathymetry Estimates

Introduction

Significant advances have been made in the use of satellite multispectral imagery for the estimation of bathymetry (Clark et al., 1988; Clark et al., 1987; Lyzenga, 1985). Extensive analysis of thematic mapper (TM) imagery, gathered on board NASA's Landsat, has shown the multiband regression model to be robust and accurate to within 1 to 2 m. Development of the airborne NOARL scanner provided multispectral data with both higher ground and spectral resolution. The TM has a 30-m ground resolution, whereas the scanner has a 1-m ground resolution (based on altitude of 500 m). Table 1 compares the scanner and TM spectral bands. Increased resolution in TM bands 1 and 2 provides more information for the scanner in the water-penetrating, blue-green bands.

A major goal of the Coastal Image Understanding project is to compare the effects of the scanner's increased resolution on bathymetry estimates with those obtained from TM imagery. This report documents the bathymetry results using multispectral data from each of the sensors compared to ground truth data obtained from a Naval Oceanographic Office (NAVOCEANO) ship survey off Key West, FL (Fig. 1).

Background

The Coastal Image Understanding project is an effort to improve the accuracy of passive shallow-water bathymetry and to classify and identify features of

Table 1. Spectral bandwidths of the scanner and the TM.

SCANNER	TM	BANDWIDTH
1	1	450 - 480 nm
2	1	480 - 520 nm
3	2	520 - 550 nm
4	2	550 - 600 nm
5	3	630 - 690 nm
6	4	760 - 900 nm
7	5	1.55 - 1.75 μm
8	6	2.08 - 2.35 μm
9	7	10.40 - 12.50 μm

naval interest in the coastal area that can directly address U.S. Navy and Defense Mapping Agency (DMA) requirements.

Past work on TM data (Clark et al., 1988) has shown that the multiband algorithm performs better than the previously tested single- and dual-band algorithms. The multiband regression model using TM gives 1- to 2-m root-mean-square (RMS) depth errors in the relatively clear waters off Key West, FL, and the island of Puerto Rico.

The development of the high-resolution multispectral scanner for the Airborne Bathymetric Survey (ABS) system produced data with 1-m resolution and finer bandwidths in the water-penetrating portion of the visible spectrum. During the field testing of the ABS system, much data was collected over the Key West area around the East Sambo Shoals, including dense hydrographic boat soundings, as well as multispectral data over the same area.

The application of the multiband algorithm to the high-resolution scanner data is of interest in determining whether that data can give better depth estimates. The availability of scanner data, along with TM data and bathymetry data in the Key West area, provided the data set for comparing the various resolution effects on depth estimates.

Procedures

Current multispectral depth algorithms are based on the functional form of the single-band radiance model (Clark et al., 1987a). Statistical regression techniques are used to determine the unknown parameters using water depths known at several pixel locations in the multispectral image. Single- and dual-band ratio models are extremely sensitive to changes in bottom reflectance and water clarity. Multiband algorithms in which the radiance and bottom reflectance are functions of the wavelength can be used to minimize difficulties encountered due to changes in the bottom reflectance and water attenuation. A development of the multiband model from the single-band radiance equation is presented here.
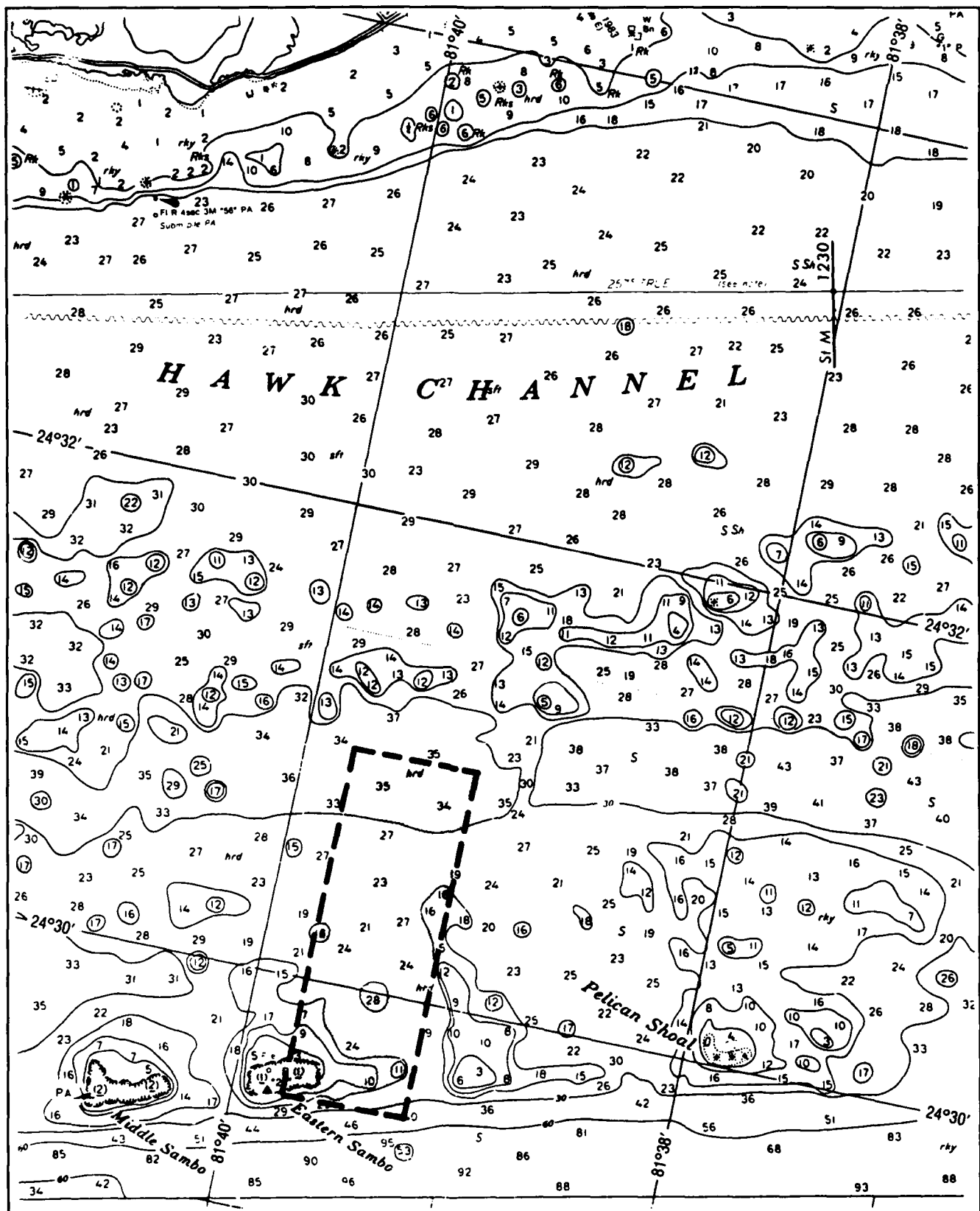
Figure 1. Study area south of Key West, FL, represented by dashed lines on 1:40000 scale NOAA chart no. 11445. Soundings are shown in feet.

The single-band radiance equation, where total radiance from the water, L_i, for a single bandwidth (i) is written as

$$L_i = L_{\infty i} + s_i\, r_i \exp[-f\,k_i\,z], \tag{1}$$

where

$L_{\infty i}$ = radiance from deep water;

s_i = a function of transmittance of air and water surface, surface refraction, and solar irradiance;

r_i = bottom reflectance;

k_i = effective attenuation coefficient of the water;

f = geometric factor to account for the pathlength through the water;

z = water depth;

$i = 1, 2 \ldots n$;

n = number of spectral bandwidths.

This model has had several implementations (Clark et al., 1987b; Paredes and Spero, 1983). Some implementations require either classifying the data into bottom cover types or knowledge of optical parameters. Other implementations use band ratios and combinations of bands. Ratios work rather well if they are constant for all bottom types in the area of interest. The ratio method was outlined by Polcyn et al. (1976) and elaborated by Lyzenga (1985). The generalized band ratio algorithm has been found to give the best results (Clark et al., 1988). A brief summary of the method is given here. Equation (1) is usually linearized and solved for z to yield

$$z = (1/fk_i)\, (ln\,[r_i] - X_i), \tag{2}$$

where $X_i = ln\,[(L_i - L_{\infty i})/s_i]$. Equation (2) can be reparameterized with $b_{0i} = (1/fk_i)\,(ln\,[r_i])$, $b_{1i} = -(1/fk_i)$, and $X_{0i} = 1$.

The depth z, for 1 channel, can the be expressed in matrix notation as $z = b'x$. The vector b contains the weights b_0 and b_1. The vector x contains $[1, x]$.

For n bandwidths, the depth z can be expressed as a weighted sum of single band terms as follows:

$$z = w_1 b_1 x_1 + w_2 b_2 x_2 + \ldots + w_n b_n x_n, \tag{3}$$

where the b and x vectors are defined as above for each band, and the ws are weights whose sum equals 1. In matrix form, this equation can be written

$$z = w'B'x, \tag{4}$$

where w is a vector of $n + 1$ weights, B is a diagonal matrix of weights where b_0 is a constant term derived from the sum of constant terms for each band, and x is an $n + 1$ vector with $x_0 = 1$. The motivation behind the summation of constant terms is given by Paredes and Spero (1983), and discussed here.

For m bottom cover types, and n bandwidths such that $m = n$, Paredes and Spero have shown that a vector c of length n exists, such that

$$c'A = 1, \tag{5}$$

where 1 is a $1's$ vector of length n and A is defined as the n by m matrix.

$$A = \begin{matrix} ln\,r_{11} & \ldots & ln\,r_{1m} \\ ln\,r_{21} & \ldots & ln\,r_{2m} \\ \cdot & \ldots & \cdot \\ \cdot & \ldots & ln\,r_{nm} \end{matrix} \tag{6}$$

Each element of A is the logarithm of the bottom reflectance term for the nth channel and the mth bottom type. As long as the number of bottom types, m, is not greater than the number of channels, n, a solution for c can be found. Paredes and Spero show that for $m = n$ bottom types, the weights w_i can be written

$$w_i = c_i k_i\, /\, c'k. \tag{7}$$

Equation 4, can be written as

$$z = w'b_0 + w'b_1 x, \tag{8}$$

where $w'b_0 = (1/f)[c'k]^{-1}\, c'A$. Since $c'A$ is 1, the bottom reflectance term vanishes, and only the sum of constant terms remains. The multiband depth model can thus be expressed independently of bottom type reflectance, as the linear regression model

$$z = \beta X + \varepsilon, \tag{9}$$

where β is the vector $w'B$ of coefficients derived from the least-squares solution of equation 3, X is the vector of reflectances, and ε is the error.

Results from comparison of the multiband model to the single-band and dual-band ratio models indicate that the multiband generalized ratio technique gives superior results and is computationally efficient as well.

Results

Comparisons were made using various channel combinations. In comparing these different spectral bandwidths for bathymetry estimation, it is useful to observe the transmittance of light through pure seawater (Fig. 2). The transmittance falls off very quickly after 575 nanometers (nm). The transmittance at wavelengths below 575 nm is greater than 90% for pure seawater. The wavelength range with the higher transmissivity will therefore be the best for depth determination. Transmittance for coastal waters shows a similar dependence but is of lower magnitude. The

3

range of wavelength bands for the two scanners is depicted by vertical bars in Figure 2.

Tests were also run using a maximum depth range to examine the depth effects on the bathymetric error estimates from the different scanners. Different band comparison results are presented as a function of maximum depth. The depth range used for each comparison always ranges from 0 m to maximum depth.

The test data set includes ship-derived depth soundings from a hydrographic survey by NAVOCEANO conducted as part of the ABS system field tests in August of 1988. The survey area extended from near 24°29.5' to 24°31'N and from 81°39.75' to 81°39.25'W. The area (Fig. 1) covers the eastern half of the Eastern Sambo shoal area and the region to the north of it. Approximately 540 depth soundings exist for the scanner and TM data sets. The depths varied from 0 to 10 m. The spacing between boat soundings (25 m) was dense due to the high ABS sampling rate. The TM data in most cases had more than one sounding per 30-m pixel. In these cases, the soundings were averaged to produce a mean depth per pixel.

Figure 3 shows the results of the multiband model using all visible bands of the TM and all visible bands of the scanner. Table 2 summarizes the results. The errors were slightly less for the scanner in the 3- to 6-m range. The differences extend from 0.36 m for waters up to 4 m deep to 0.03 m for waters up to 6 m deep. Differences for depths beyond 6 m were not significant. Both data sets showed an upward trend
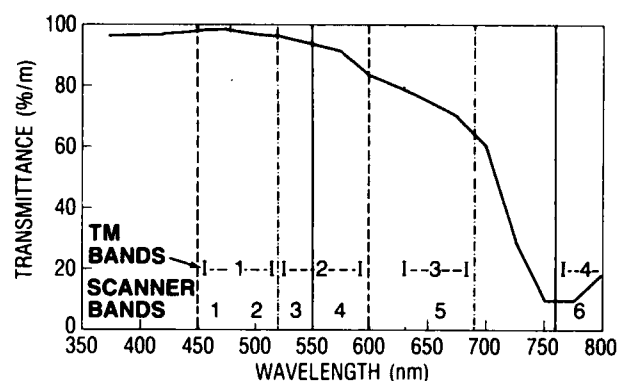

Figure 2. Optical transmittance of pure seawater versus wavelength (after Jerlov, 1968). TM and scanner bandwidths shown by vertical lines. (Transmittance for coastal waters shows a similar dependence but is between 5 and 10% lower in magnitude.)
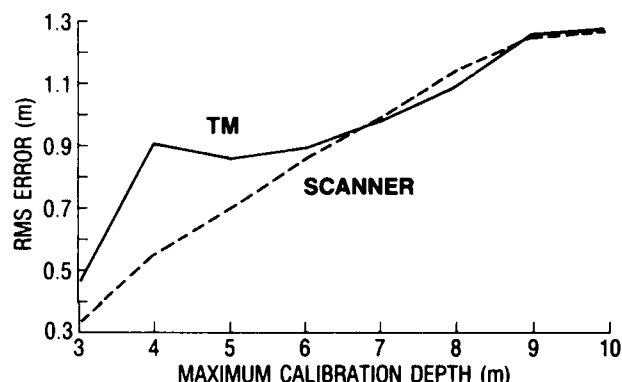

Figure 3. Comparison of errors in bathymetry estimation between scanner bands 1, 2, 3, 4, 5 and TM bands 1, 2, 3.

Table 2. Summary of scanner (S) and TM bathymetry estimates using TM bands 1, 2, 3, and S bands 1, 2, 3, 4, 5. Errors in meters.

MAXIMUM DEPTH	REGR. R**2	NUMBER CALIB	POINTS TEST	MEAN ERROR	RMS ERROR
S 10	0.701	270	269	0.079	1.270
TM 10	0.645	147	147	-0.148	1.284
S 9	0.692	265	265	0.075	1.252
TM 9	0.643	143	144	-0.145	1.261
S 8	0.670	236	234	0.079	1.143
TM 8	0.629	118	119	-0.183	1.092
S 7	0.602	190	190	-0.0005	0.986
TM 7	0.676	82	93	-0.046	0.976
S 6	0.633	142	140	-0.097E-05	0.855
TM 6	0.797	58	58	-0.112	0.890
S 5	0.603	73	73	0.058	0.691
TM 5	0.686	24	26	-0.192	0.858
S 4	0.631	38	40	0.062	0.544
TM 4	0.760	14	15	-0.083	0.907
S 3	0.881	12	12	-0.954E-06	0.323
TM 3	0.941	6	6	-0.333	0.449

in the RMS error with increasing depth. Scanner error increased steadily and leveled off around 9 m. TM error seemed to increase more rapidly in the shallower waters between 3 and 5 m and followed the same trend as the scanner after 6 m.

The mean residual error is plotted in Figure 4. The TM showed a consistent negative bias. Since the errors are cumulative, it was believed the errors at the 3-m level were weighting the errors at the higher depths downward; however, the error at 3 m was based on only 6 points. The error at 10 m is based on 147 test points. It is possible that the L_∞ values used were too low. The errors for the scanner were less erratic and less biased and were constrained between 0 and 0.08 m. The errors for the TM, however, were between -0.05 and -0.20 m (excludes 3-m error). The errors did not show trends.

In addition to the all-band comparisons, different band combinations were compared. As shown in Table 1, scanner bands 1 and 2 cover the same spectral bandwidth as TM band 1, and scanner bands 3 and 4 cover the same spectral bandwidth as TM band 2. Scanner band 5 is equivalent to TM band 3; therefore, combinations of the scanner bands were tested against the TM bands. Test results are shown in Tables 3 and 4, and error plots are shown in Figures 5 and 6. Results of the two-band and four-band runs for the scanner did not differ greatly, mainly due to the high correlation between the blue and green bands. Figure 7 shows scatter plots of various band combinations in which the high degree of correlation can be seen. The best results from the two-band combinations came from bands 2 and 4. The five-band results were slightly but not significantly better than the two-band results. Comparison with the TM bands showed similar results to the all-band comparisons, with better results from the scanner in the 3- to 6-m range, and no significant differences beyond 7 m.

Figure 8a shows the TM true-color image with the scanner coverage area outlined in red (Fig. 8b). Figure 9 shows the true-color image of the raw scanner
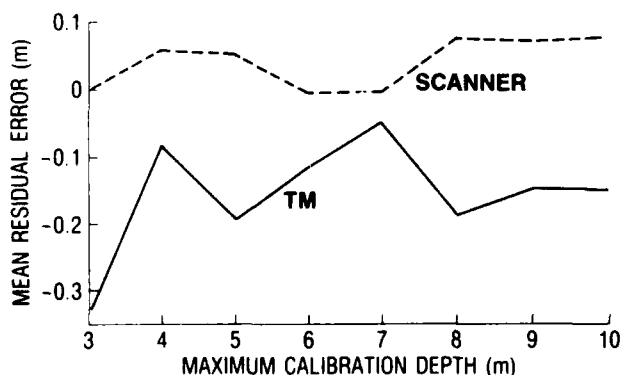
data for the area outlined in Figure 8b. Figures 10 and 11 show bathymetry contours from the TM and scanner data sets, respectively.

The wider scanner bands that correspond to the TM are used to compare ground resolution effects. Scanner bands 2 and 4 are compared with TM bands 1 and 2. The result is the same as that reported for the two-band comparisons shown in Figure 5.

Summary and Conclusions

TM and scanner data were compared. The scanner data were better than the TM data in the shallow area between 3 and 6 m. Comparisons of the scanner data at different resolutions is planned to differentiate the combined effect of increased spectral and spatial resolution.

The improvement in data by using the scanner was less than expected and is attributed to several factors. First, the scanner's higher spatial resolution is much more sensitive to horizontal registration errors than the lower resolution TM. The integrated response over the lower resolution TM and the averaging of soundings within the 30-m cell area could give
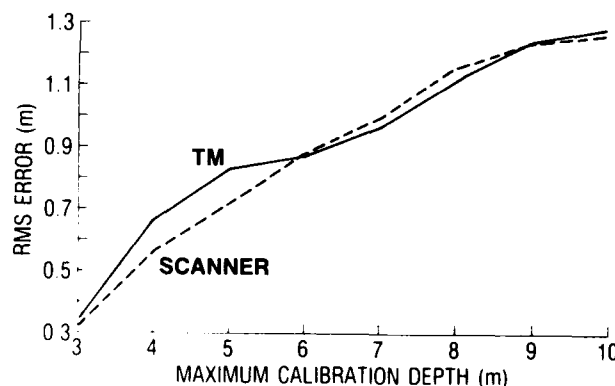
Figure 5. Comparison of errors in bathymetry estimation between scanner bands 2, 4, and TM bands 1, 2.
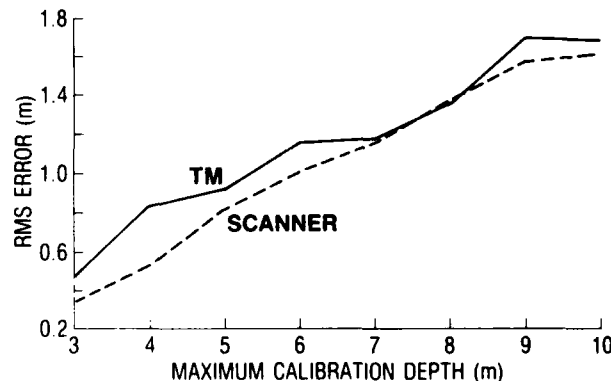
Figure 6. Comparison of errors in bathymetry estimation between scanner bands 4, 5 versus TM bands 2, 3.

Figure 4. Plot of mean residual error for scanner and TM.

5

Table 3. Summary of scanner (S) and TM bathymetry estimates using TM bands 1 and 2 and S bands 1, 2, 3, and 4. Errors in meters.

DEPTH	SENSOR/BANDS	RMUL	(ACTUAL-CALCULATED) MEAN	RMS	# CALIB POINTS	# TEST POINTS
0-3	S/13	0.587	-0.4167E-01	0.3200	12	12
	S/14	0.843	-0.9537E-06	0.3227	12	12
	S/23	0.666	-0.8333E-01	0.3118	12	12
	S/24	0.828	-0.9537E-06	0.3227	12	12
	TM/12	0.887	-0.1167	0.3436	6	6
0-4	S/13	0.374	-0.9537E-06	0.5701	38	40
	S/14	0.605	0.8750E-01	0.5743	38	40
	S/23	0.170	-0.1250E-01	0.4998	38	40
	S/24	0.488	0.5000E-01	0.5679	38	40
	TM/12	0.561	-0.1167	0.6700	14	15
0-5	S/13	0.457	0.1027E-01	0.7590	73	73
	S/14	0.593	0.7877E-01	0.6785	73	73
	S/23	0.264	-0.1027E-01	0.8516	73	73
	S/24	0.484	0.7877E-01	0.7225	73	73
	TM/12	0.685	-0.1923	0.8358	24	26
0-6	S/13	0.460	-0.6429E-01	0.9790	142	140
	S/14	0.614	-0.3929E-01	0.8368	142	140
	S/23	0.398	-0.2143E-01	1.204	142	140
	S/24	0.604	-0.1429E-01	0.8833	142	140
	TM/12	0.788	-0.6035E-01	0.8751	58	58
0-7	S/13	0.430	0.7894E-02	1.168	190	190
	S/14	0.588	-0.1053E-01	1.004	190	190
	S/23	0.384	0.2631E-01	1.220	190	190
	S/24	0.570	0.1579E-01	0.9943	190	190
	TM/12	0.663	-0.5645E-01	0.9645	82	93
0-8	S/13	0.469	0.3205E-01	1.351	236	234
	S/14	0.656	0.6624E-01	1.186	236	234
	S/23	0.419	0.1068E-01	1.345	236	234
	S/24	0.633	0.5555E-01	1.159	236	234
	TM/12	0.627	-0.1786	1.120	118	119
0-9	S/13	0.502	0.6509E-01	1.459	265	265
	S/14	0.681	0.6887E-01	1.293	265	265
	S/23	0.420	0.4245E-01	1.485	265	265
	S/24	0.638	0.3113E-01	1.243	265	265
	TM/12	0.643	-0.1389	1.245	143	144
0-10	S/13	0.518	0.6227E-01	1.484	270	269
	S/14	0.690	0.6970E-01	1.301	270	269
	S/23	0.432	0.4740E-01	1.514	270	269
	S/24	0.646	0.6041E-01	1.269	270	269
	TM/12	0.645	-0.1378	1.285	147	147

improved estimates on the order of the square root of the number of soundings. The higher number of bands does not seem to offer much improvement due to the high amount of collinearity between them. However, the finer spectral bandwidths can be used to advantage in different types of ocean water, since the attenuation and absorption properties are optimal at different wavelengths.

Table 4. Summary of scanner (S) and TM bathymetry estimates using TM bands 2 and 3 and S bands 3, 4 and 5. Errors in meters.

| DEPTH	SENSOR/BANDS	RMUL	(ACTUAL-CALCULATED) MEAN	RMS	# CALIB POINTS	# TEST POINTS
0-3	S/35	0.574	-0.9537E-06	0.3227	12	12
	S/45	0.756	-0.4167E-01	0.3200	12	12
	TM/23	0.931	-0.3333	0.4488	6	6
0-4	S/35	0.165	-0.9537E-06	0.5244	38	40
	S/45	0.305	-0.1250E-01	0.5122	38	40
	TM/23	0.614	0.1167	0.8260	14	15
0-5	S/35	0.207	-0.3767E-01	0.7935	73	73
	S/45	0.179	-0.2397E-01	0.8111	73	73
	TM/23	0.359	-0.1154	0.9152	24	26
0-6	S/35	0.211	-0.6786E-01	1.504	142	140
	S/45	0.311	-0.1179E-00	1.006	142	140
	TM/23	0.617	-0.1638	1.153	58	58
0-7	S/35	0.273	-0.7896E-02	1.217	190	190
	S/45	0.357	-0.2632E-01	1.153	190	190
	TM/23	0.550	-0.2957E-01	1.177	82	93
0-8	S/35	0.322	-0.1710E-01	1.424	236	234
	S/45	0.430	-0.2351E-01	1.373	236	234
	TM/23	0.410	-0.1618	1.358	118	119
0-9	S/35	0.285	0.3868E-01	1.651	265	265
	S/45	0.362	-0.9444E-03	1.584	265	265
	TM/23	0.158	-0.9722E-01	1.705	143	144
0-10	S/35	0.281	0.1208E-01	1.671	270	269
	S/45	0.348	-0.4648E-02	1.621	270	269
	TM/23	0.142	-0.1173	1.698	147	147
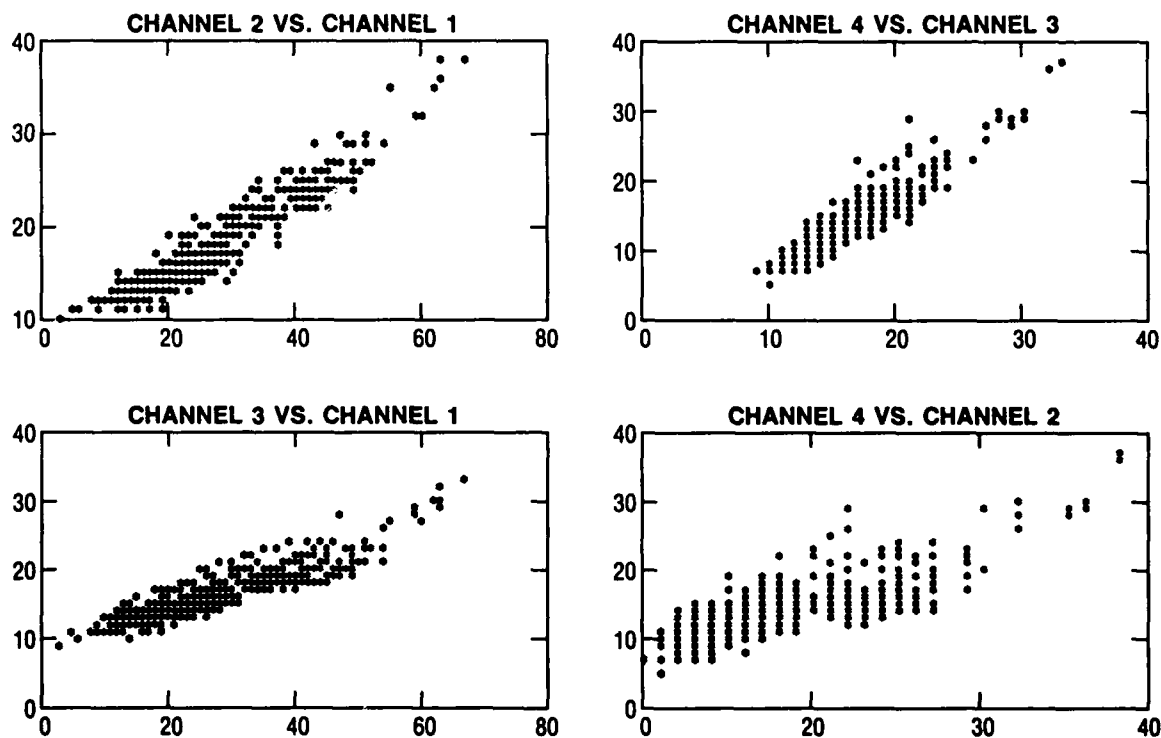
Figure 7. Scatter plots of scanner channels showing the correlation between the blue and green bands for different combinations.
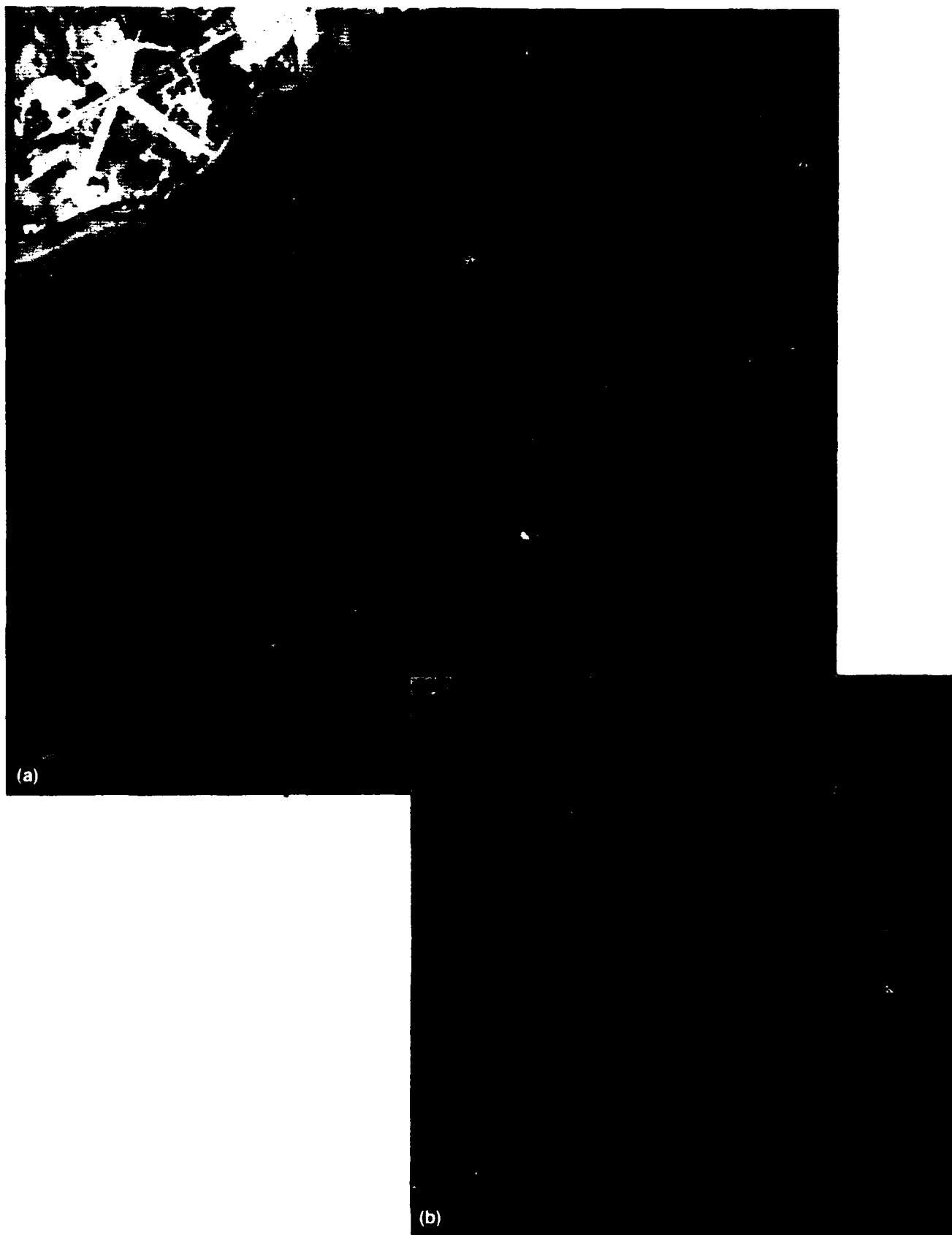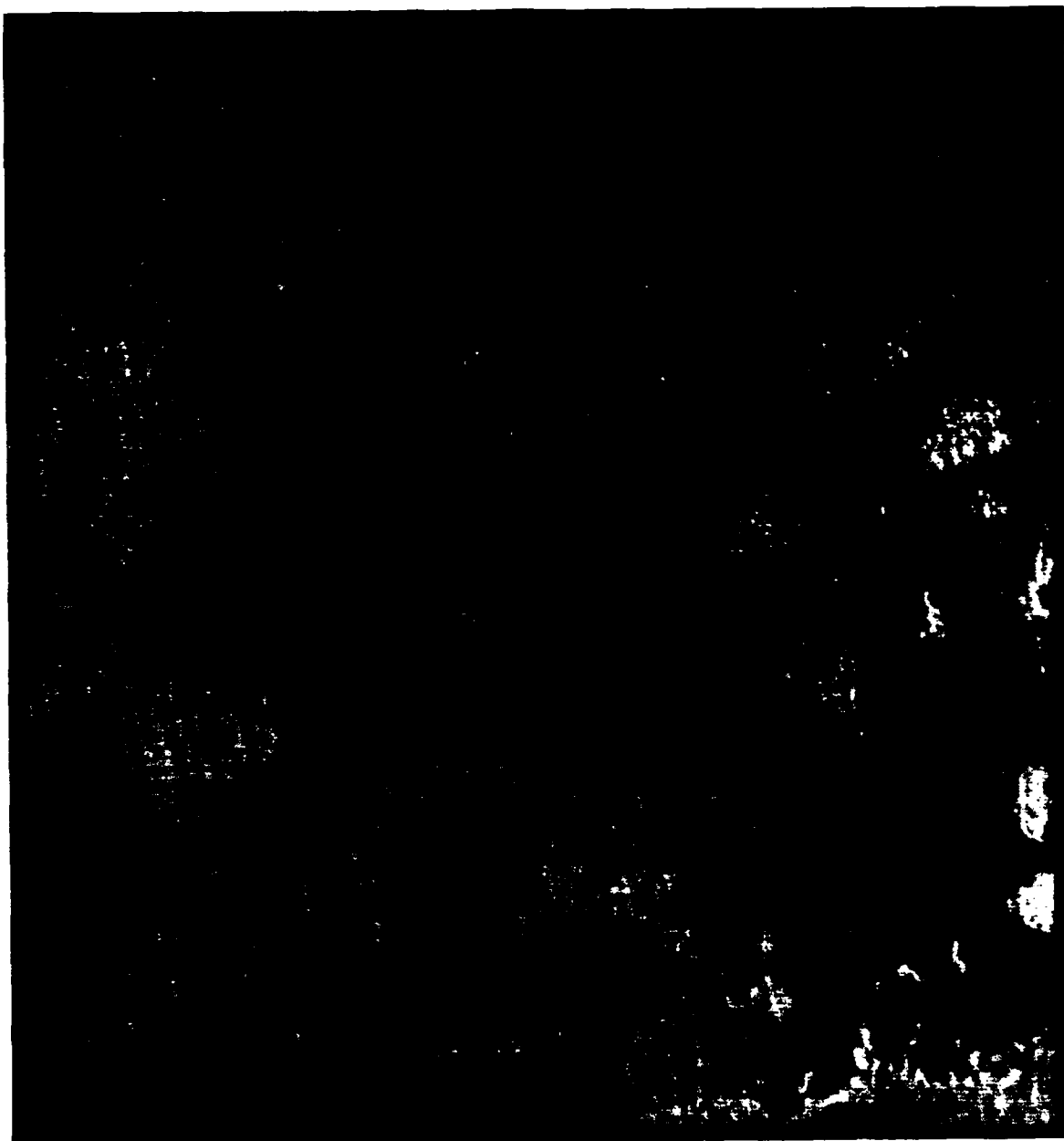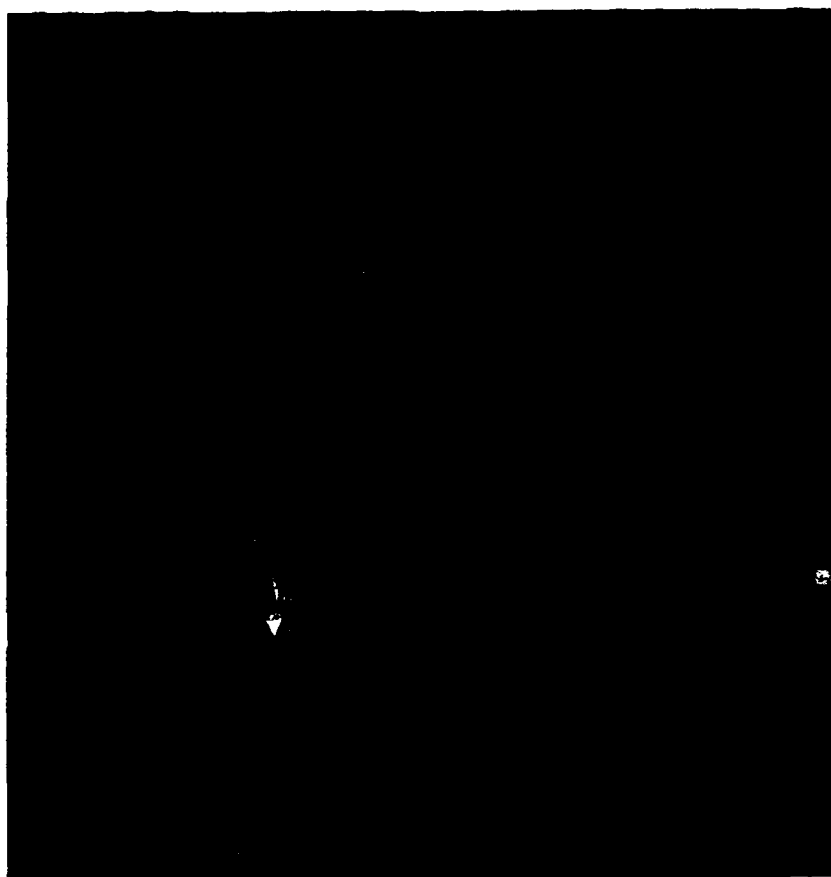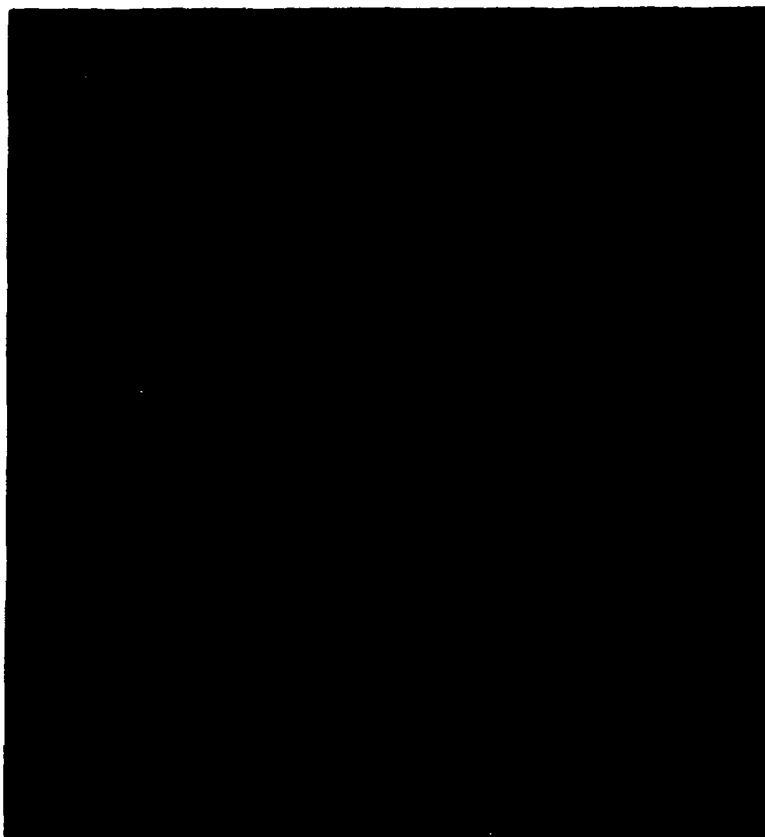
7

Figure 8. (a) TM image of Key West, Fl. (b) Study area outlined in red.

Figure 9. *True-color image of Key West, FL, from scanner.*

Figure 10. Bathymetric color contours at 1-m spacing derived from TM.

Figure 11. Bathymetric color contours at 1-m spacing derived from scanner.

Recommendations

Recommendations for future work are to collect data in an area with a homogeneous bottom, such as sand, to minimize errors due to rapidly changing bottom types. The registration of 1-m resolution scanner data to a rapidly changing bottom requires very high precision positioning data. The limited availability of GPS satellites during the collection of the scanner data did not yield the best satellite configuration for the precise positioning needed. A slowly changing bottom, where most of the variability is from depth variations and not from cover type changes, would be more robust to registration errors.

Research also needs to be done to see if surface characteristics, derivable from glint patterns on the surface in the multispectral data, can be used to improve bathymetry estimation. Surface waves can provide some information about the nature of the bottom, which might then be used to help distinguish depth variations from bottom type variations. This distinction could provide better depth accuracy from the multiband model in areas where bottom type variability is a problem.

For areas of the world where surveying is denied, the application of bathymetry collection techniques from multispectral data could yield products descriptive of coastal zone variability, surf-induced beach erosion, shoal emergence areas, and possible shipping routes. Although bathymetry can be accurately described only to 3-m depths (by International Hydrographic Office standards) with the scanner, satellite-derived bathymetry can be valuable for planning purposes in areas where no data are available.

References

Clark, K. R., T. H. Fay, C. L. Walker (1988). Bathymetry using thematic mapper imagery. *SPIE Ocean Optics IX*, Orlando, Florida, April.

Clark, K. R., T. H. Fay, and C. L. Walker (1987a). Bathymetry calculations with Landsat 4 thematic mapper imagery under a generalized ratio assumption. *Applied Optics* 26(19):4036-4038.

Clark, K. R., T. H. Fay, and C.L. Walker, (1987b) *A Comparison of Models for Remotely Sensed Bathymetry,* Naval Ocean Research and Development Activity, Stennis Space Center, MS, NORDA Report 145, August.

Jerlov, N. G. (1968). *Optical Oceanography*, New York, Elsevier.

Lyzenga, D. R. (1985). Shallow-water bathymetry using combined lidar and passive multispectral scanner data. *Remote Sensing.* 6(1): 115-125.

Paredes, J. M., R. E. Spero, (1983). Water depth mapping from passive remote sensing data under a generalized ratio assumption. *Applied Optics.* 22(8): 1134-1135.

Polcyn, F. C. (1976). *NASA/Cousteau Ocean Bathymetry Experiment-Remote Bathymetry Using High Gain Landsat Data*, NASA CR-ERIM 118500-1-F, NASA Goddard Space Flight Center, July.

Distribution List

Applied Physics Laboratory
Johns Hopkins University
John Hopkins Road
Laurel MD 20707

Applied Physics Laboratory
University of Washington
1013 NE 40th St.
Seattle WA 98105

Applied Research Laboratory
Pennsylvania State University
P.O. Box 30
State College PA 16801

Applied Research Laboratory
University of Texas at Austin
P.O. Box 8029
Austin TX 78713-8029

Assistant Secretary of the Navy
Research, Engineering & Systems
Washington DC 20350-2000

Chief of Naval Operations
Washington DC 20350-2000
Attn: OP-71
OP-987

Chief of Naval Operations
Oceanographer of the Navy
Washington DC 20392-1800
Attn: OP-096
OP-96B

David W. Taylor Naval Research Center
Bethesda MD 20084-5000
Attn: Commander

Defense Mapping Agency
Systems Center
12100 Sunset Hill Rd #200
Reston VA 22090-3207
Attn: Director
Code SGWN

Director of Navy Laboratories
Crystal Plaza #5, Rm. 1062
Washington DC 20360

Fleet Antisub Warfare Tng Ctr-Atl
Naval Station
Norfolk VA 23511-6495

Fleet Numerical Oceanography Center
Monterey CA 93943-5005
Attn: Commanding Officer

National Ocean Data Center
1825 Connecticut Ave., NW
Universal Bldg. South, Rm. 406
Washington DC 20235
Attn: G. Withee, Director

Naval Air Development Center
Warminster PA 18974-5000
Attn: Commander

Naval Air Systems Command HQ
Washington DC 20361-0001
Attn: Commander

Naval Civil Engineering Laboratoray
Port Hueneme CA 93043
Attn: Commanding Officer

Naval Coastal Systems Center
Panama City FL 32407-5000
Attn: Commanding Officer

Naval Facilities Engineering
Command HQ
200 Stovall St.
Alexandria VA 22332-2300
Attn: Commander

Naval Oceanographic Office
Stennis Space Center MS 39529
Attn: Commanding Officer

Naval Oceanography Command
Stennis Space Center MS 39529
Attn: Commander

Naval Oceanographic & Atmospheric
Research Laboratory
Stennis Space Center MS 39529-5004
Attn: Code 100
Code 110
Code 105
Code 115
Code 125L (10)
Code 125P
Code 200
Code 300
Code 400

Naval Oceanographic & Atmospheric
Research Laboratory
Liaison Office
Crystal Plaza #5, Rm. 802
Arlington VA 22202-5000
Attn: B. Farquhar

Naval Ocean Systems Center
San Diego CA 92152-5000
Attn: Commander

Naval Postgraduate School
Monterey CA 93943
Attn: Superintendent

Naval Research Laboratory
Washington DC 20375
Attn: Commanding Officer

Naval Sea Systems Command HQ
Washington DC 20362-5101
Attn: Commander

Naval Surface Warfare Center
White Oak
10901 New Hampshire Ave.
Silver Spring MD 20904-5000
Attn: Commander
Library

Naval Surface Weapons Center
Dahlgren VA 22338-5000
Attn: Commander

Naval Underwater Systems Center
Newport RI 02841-5047
Attn: Commander

Naval Underwater Systems Center Det
New London Laboratory
New London CT 06320
Attn: Officer in Charge

Office of Naval Research
800 N. Quincy St.
Arlington VA 22217-5000
Attn: Code 10D/10P, Dr. E. Silva
Code 112, Dr. E. Hartwig
Code 12
Code 10

Office of Naval Research
ONR Branch Office
Box 39
FPO New York 09510-0700
Attn: Commanding Officer

Office of Naval Technology
800 N. Quincy St.
Arlington VA 22217-5000
Attn: Code 20, Dr. P. Selwyn
Code 228, Dr. M. Briscoe
Code 234, Dr. C. Votaw

Scripps Institution of Oceanography
University of California
P.O. Box 6049
San Diego CA 92106

Space and Naval Warfare
Systems Command
Washington DC 20363-5100
Attn: Commander

Woods Hole Oceanographic Institution
P.O. Box 32
Woods Hole MA 02543
Attn: Director

REPORT DOCUMENTATION PAGE

Public reporting burden for this collection of information is estimated to average 1 hour per response, including the time for reviewing instructions, searching existing data sources, gathering and maintaining the data needed, and completing and reviewing the collection of information. Send comments regarding this burden estimate or any other aspect of this collection of information, including suggestions for reducing this burden, to Washington Headquarters Services, Directorate for Information Operations and Reports, 1215 Jefferson Davis Highway, Suite 1204, Arlington, VA 22202-4302, and to the Office of Management and Budget, Paperwork Reduction Project (0704-0188), Washington, DC 20503.

1. Agency Use Only (Leave blank).	2. Report Date. June 1990	3. Report Type and Dates Covered. Final

4. Title and Subtitle.

Comparison of Thematic Mapper and NOARL Scanner Multispectral Bathymetry Estimates

6. Author(s).

Maria T. Kalcic, Charles L. Walker, and Harold V. Miller

5. Funding Numbers.

Program Element No. 62435N

Project No. RM035

Task No. G85

Accession No. DN255031

7. Performing Organization Name(s) and Address(es).

Ocean Science Directorate
Naval Oceanographic and Atmospheric Research Laboratory
Stennis Space Center, Mississippi 39529-5004

8. Performing Organization Report Number.

NOARL Report 4

9. Sponsoring/Monitoring Agency Name(s) and Address(es).

10. Sponsoring/Monitoring Agency Report Number.

11. Supplementary Notes.

12a. Distribution/Availability Statement.

Approved for public release; distribution is unlimited. Naval Oceanographic and Atmospheric Research Laboratory, Stennis Space Center, Mississippi 39529-5004.

12b. Distribution Code.

13. Abstract (Maximum 200 words).

The Mapping, Charting, and Geodesy Division of the Naval Oceanographic and Atmospheric Research Laboratory (NOARL) investigates methods to exploit the application of multispectral data to coastal water mapping and charting requirements. The Coastal Image Understanding project high-resolution, multispectral, aircraft data has been examined and compared with lower-resolution satellite data from the thematic mapper on board NASA's Landsat. The high-resolution, nine-band scanner used was developed for the Airborne Bathymetric Survey System. The NOARL scanner has increased spectral sensitivity in the blue and green portions of the electromagnetic spectrum to take advantage of the water-penetrating bands. The multiband generalized ratio model is used to compare bathymetry estimates from the scanner and the thematic mapper, which has five bands. Results show improvement from increased resolution in the 3-m to 6-m area. Root-mean-square (RMS) errors of 0.323 m at the 3-m depth range for the NOARL Scanner are close to the International Hydrographic Office standard of 0.3 m; however, errors at other depth ranges exceed this standard by even greaters values. RMS errors of 0.544 m for the NOARL scanner contrast with 0.907 m for the thematic mapper at the 4-m range. Beyond 6-m depth, results do not differ significantly between the two scanners.

14. Subject Terms.

hydrography, bathymetry, optical properties, optical detectors

15. Number of Pages. 15

16. Price Code.

17. Security Classification of Report.	18. Security Classification of This Page.	19. Security Classification of Abstract.	20. Limitation of Abstract.
Unclassified	Unclassified	Unclassified	None